Received 19 December 2017; revised 23 April 2018; accepted 15 June 2018. Date of publication 21 June 2018;
date of current version 6 July 2018. The review of this paper was arranged by Editor S. Chakrabarti.

Digital Object Identifier 10.1109/JEDS.2018.2849393

Investigating on Through Glass via Based RF Passives for 3-D Integration

LIBO QIAN [1] (Member IEEE), JIFEI SANG[1], YINSHUI XIA[1], JIAN WANG [1], AND PEIYI ZHAO[2]

1 Faculty of Electrical Engineering and Computer Science, Ningbo University, Ningbo 315211, China
2 School of Computational Science, Chapman University, Orange, CA 92866 USA

CORRESPONDING AUTHOR: L. QIAN (e-mail: qianlibo@nbu.edu.cn)

This work was supported in part by the National Natural Science Foundation of China under Grant 61771268, Grant U1709218, Grant 61571248, and Grant 61671257, in part by the Science and Technology Fund of Zhejiang Province under Grant 2015C31090, in part by the Natural Science Foundation of Zhejiang under Grant LY17F040002, and in part by the work of K. C. W. Magna Fund in Ningbo University.

ABSTRACT Due to low dielectric loss and low cost, glass is developed as a promising material for advanced interposers in 2.5-D and 3-D integration. In this paper, through glass vias (TGVs) are used to implement inductors for minimal footprint and large quality factor. Based on the proposed physical structure, the impact of various process and design parameters on the electrical characteristics of TGV inductors is investigated with 3-D electromagnetic simulator HFSS. It is observed that TGV inductors have identical inductance and larger quality factor in comparison with their through silicon via counterparts. Using TGV inductors and parallel plate capacitors, a compact 3-D band-pass filter (BPF) is designed and analyzed. Compared with some reported BPFs, the proposed TGV-based circuit has an ultra-compact size and excellent filtering performance.

INDEX TERMS Through glass via inductor, integrated passive device, band-pass filter, 3-D integration.

I. INTRODUCTION

Through silicon via (TSV) based three dimensional integration is considered to be a promising alternative beyond Moore's Law, in which TSVs are formed as vertical signal, power and thermal paths. Due to less area and high integration density, TSVs are also proposed as radio frequency (RF) passive components, such as TSV inductors and capacitors [1], [2]. However, TSVs in silicon interposers suffer from high electrical loss and high processing cost. To address these issues, glass is proposed as a compelling alternative to silicon interposers.

In comparison with silicon interposers, glass provides ultrahigh electrical resistivity, which makes TGVs own low electrical loss. Moreover, TGVs can be fabricated using low-cost panel processes and do not need to use via liners for electrical isolation [3]. Because of these advantages, TGVs have been studied aggressively. Tong *et al.* [4] proposed a wideband scalable circuit model for tapered through package vias in glass interposers. Cho *et al.* [5] experimentally and numerically investigated the impact of copper TGVs on the thermal performance of glass interposers. Based on TGV technology, Wei *et al.* [6] designed two compact waveguide structures and analyzed the transmission characteristics of these structures. Using the TGV as a min radiator, Hwangbo *et al.* [7] developed a directional TGV antenna for wireless point to point communication. Hsieh *et al.* [8] and Kim *et al.* [9] fabricated and measured through glass via RF inductors, respectively. The impact of turn number on the quality factor performance and inductance density was characterized in [9]. In addition to the number of turns, the performance of 3D inductors depends on other factors, such as via diameter, interposer height, via pitch and redistribution line parameters. These factors are taken into consideration when optimizing the inductor performance. Moreover, fewer researches have addressed the applications of the 3-D inductors in RF circuit design.

This study proposes the physical structure of TGV inductor and analyzes the impact of various process and design parameters on the inductance and quality factor of the inductor. Using TGV inductors and parallel plate capacitors, a TGV based 3-D band pass filter is designed and compared.

II. ELECTRICAL CHARACTERIZATION

Fig. 1 shows the physical structure of TGV-based inductor, which mainly consists of three parts: the TGVs, the top redistribution lines (RDLs) and the bottom RDLs. The basic parameters of the inductor are listed in Table 1 and the value of inductance L and quality factor Q can be obtained based on Y parameters from full wave electromagnetic simulator (HFSS) [10]. In comparison with planar spiral structure, a distinct advantage of such a TGV inductor is the minimal footprint area and corresponding high inductance density. Moreover, the magnetic flux of the 3-D inductor run in parallel with the on-chip horizontal metal wires, therefore, the patterned ground shield technique used in 2-D planar inductor structure [11] for reducing EM interference is not required.

$$L = Im\left(1/Y_{11}\right)/2\pi f \tag{1}$$

$$Q = Im\left(1/Y_{11}\right)/Re\left(1/Y_{11}\right) \tag{2}$$

TABLE 1. Basic parameters of TGV inductor for electrical characterization.

	Description	Symbol	Value
Process	TGV diameter	D	10μm
	Interposer thickness	L	100μm
	RDL height	H	2μm
	Relative dielectric constant/ Dielectric loss tangent of glass interposer	$\varepsilon_r / tan\delta$	6.7/0.006
Design	Turn number	N	4
	Loop pitch	P	50μm
	RDL width	W	6μm

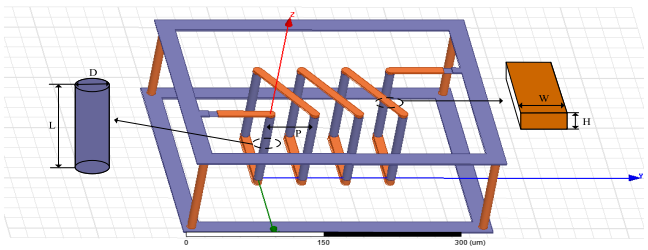

FIGURE 1. Physical structure of TGV inductor.

Based on the proposed structure, the electrical performance of the TGV-based inductor is firstly analyzed and compared. From the results shown in Fig. 2, it is observed that the inductance value of the TGV inductor is about 1.4nH and the corresponding inductance density is 80nH/mm^2, which is comparable with its TSV counterpart and offers a 15x improvement over equivalent lateral inductors in [12]. Moreover, due to small dielectric constant and low dielectric tangent, the quality factor of the TGV inductor is significantly larger than that of TSV inductor on a common silicon (silicon resistivity $\rho = 100\Omega$-cm) and is closed to that of TSV inductor on a more expensive high resistivity silicon ($\rho = 1000\Omega$-cm), which demonstrates the potential of TGV inductors in RF integrated passive device applications.

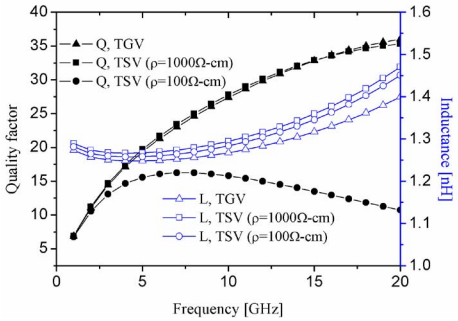

FIGURE 2. Comparison of quality factor and inductance of TGV inductors and TSV inductors.

The impact of various technical parameters, including TGV diameter, interposer thickness, TGV pitch and the number of turns on the quality factor and inductance of TGV inductors is further investigated, hoping to aid guide making in TGV inductors design and fabrication.

Fig. 3 (a) shows the impact of TGV diameter on the quality factor and inductance of TGV inductors. Similar to solenoid inductors, the inductance of TGV inductors is mainly determined by external inductance L_{out}($L_{out} = \mu NA/P$, where μ, N, A and P are the magnetic permeability, the number of turns, cross-sectional area and TGV pitch) [13]. The increase in TGV diameter decreases cross-sectional area of TGV inductors and therefore inductance values. The quality factor of inductors is defined as the ratio of the effective reactance X_L ($X_L = \omega L$, ω is angular frequency) to the frequency-dependent AC resistance (R_{ac}). The increase in TGV diameter decreases via resistance and ohmic loss; therefore, it can be seen that the quality factor increases with TGV diameter and the slope is larger at high frequency region, in which the eddy current loss and skin loss are significantly reduced.

In a 3D interposer approach, TGVs are used to realize the high density interconnections between the devices on one side of the interposer and the devices on the other side. The increase in interposer thickness increases TGV height and effective cross-sectional area of TGV inductors; therefore, it can be seen that the inductance significantly increases with interposer thickness. As illustrated in Fig. 3 (b), interposer thickness varies from 60μm to 120μm, the inductance increases by 98.5%. Moreover, it is observed that the quality factor of TGV inductors increases with interposer thickness. The reason behind this is that the increase in reactance X_L is more significant than that in AC resistance R_{ac}.

Fig. 3 (c) shows the impact of the number of turns on the quality factor and inductance of TGV inductors. As mentioned above, the external inductance of coils L_{out} is proportional to the number of turns N; therefore, it is observed that the inductance of TGV inductors significantly increases with turn number, while the variation of the quality factor with turn number is very small. The results are consistent with the measure data in [9].

For a fixed number of turns, the increase in TGV pitch increases TGV inductor length (N×P) and decreases the

inductance. As illustrated in Fig. 3 (d), TGV pitch varies from 50μm to 80μm, the inductance value decreases by 56%. On the other hand, the increase in TGV pitch also decreases the inductive coupling due to proximity effect and AC resistance R_{ac}. Finally, the variation of the quality factor with TGV pitch is very small.

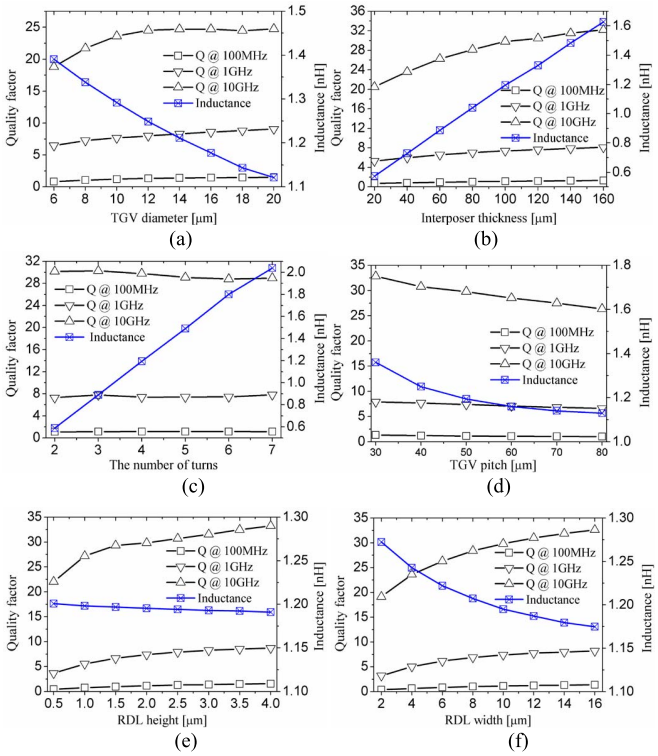

FIGURE 3. Impact of (a) TGV diameter, (b) interposer thickness, (c) the number of turns (d) TGV pitch, (e) RDL height and (f) RDL width on the quality factor and inductance of TGV inductors.

The horizontal RDL is an important part of 3-D inductors. As shown in Fig. 3 (e) and Fig. 3 (f), the impact of RDL height and RDL width on the quality factor and inductance of TGV inductors is investigated. Because the increase in RDL height and width has a modest impact on the cross-sectional area of coil inductors, it is observed that the inductance *L* varies slightly as the two parameters increase. For quality factor, the increase in RDL height and width decreases the equivalent resistance of inductors; therefore it can be seen that the quality factor of 3-D inductors increases as RDL height and width increase.

III. TGV BASED BAND PASS FILTER

Using 3D TGV inductors mentioned above and parallel plate capacitors, a compact 2nd order coupled-resonator band pass filter for 2.4-GHz WLAN application is designed in this section. As shown in Fig. 4, the filter consists of two LC resonators and three admittance inverters, in which the input inverters J_{01} and output inverter J_{23} are represented by L-type networks for impedance transformation purpose and the capacitive inverter between the resonator pairs J_{12} can be represented by a π-type

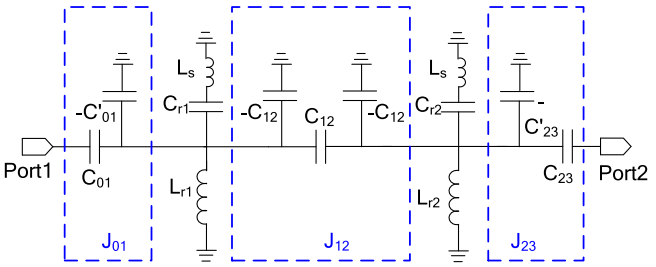

FIGURE 4. The proposed 2nd order coupled resonator band-pass filter.

network as a coupling mechanism. C_{01}, C_{12} and C_{23}areinput matching capacitor, coupling capacitor and output matching capacitor, respectively. The central frequency and pass-band can be tuned by varying the resonator components (L_r and C_r). To obtain a good roll-off characteristic, an additional upper stop-band transmission zero is inserted by adding a series inductive element (L_s) in LC resonators.

According to filter specifications for WLAN applications, the filter should have a central frequency of 2.45GHz with an operational bandwidth of more than 100MHZ. The corresponding component values are then determined as follows: the g_i value that gives a pass-band ripple of 0.5dB is selected as $g_0 = 1$, $g_1 = 1.4029$, $g_2 = 0.7071$ and $g_3 = 1.9841$ [14]. With (3)-(4) [15], the admittances of K/J inverters are then calculated as $J_{01} = 0.0125$, $J_{12} = 0.0111$, and $J_{23} = 0.0125$. Here $\omega_0 = 2\pi f_0$, $f_0$is the central frequency of the pass band. FBW is the filter fractional width and characteristic impedance $Z_0 = 50\Omega$. The value of resonant inductor L_r is set to be 1.2nH, which is a reasonable value for 3-D inductors implementation. For 2.45GHz resonant frequency, the value of resonator capacitor C_r should be 3.5pF.

$$J_{01} = \sqrt{\frac{FBW}{\omega_0 L_r g_0 g_1 Z_0}} \tag{3}$$

$$J_{12} = \frac{FBW}{\omega_0 L_r \sqrt{g_1 g_2}} \tag{4}$$

Using the closed formulas in (5), (6) and (7), the other component values are finally given as, $C_{01} = C_{23} = 1.10$pF, $C'_{01} = C'_{23} = 0.63$pF and $C_{12} = 0.65$pF.

$$C_{01} = C_{23} = \frac{J_{01}}{\omega_0 \sqrt{1 - (J_{01} Z_0)^2}} \tag{5}$$

$$C'_{01} = C'_{23} = \frac{C_{01}}{1 + (\omega_0 C_{01} Z_0)^2} \tag{6}$$

$$C_{12} = \frac{J_{12}}{\omega_0} \tag{7}$$

Based on the above parameters, the simplified lumped circuit model of the 2nd coupled resonator band-pass filter is proposed, as shown in Fig. 5 (a). Here C_r'=C_r-C'_{01}-C'_{12}, which means the negative capacitor is absorbed into the resonator capacitor C_r. According to the decided schematic, the physical layout of the proposed filter is then derived. As illustrated in Fig. 5 (b), the resonant inductors and series elements are

realized by TGV inductors and grounding via holes, respectively. The shunt-to-ground and coupled capacitors are both formed by the parallel plate structures. The resulting filter has an overall size of $440\mu m \times 330\mu m \times 150\mu m$.

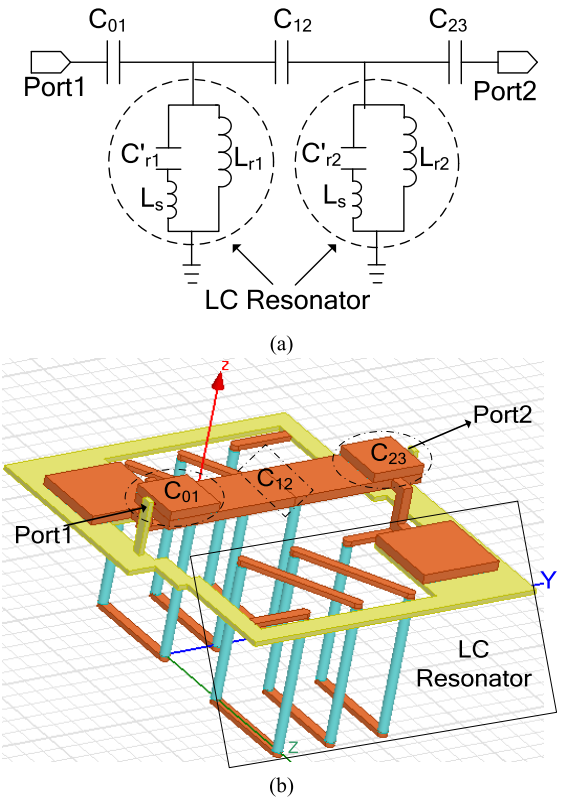

FIGURE 5. **(a) Simplified lumped circuit model and (b) 3-D layout of the proposed 2.45GHz band-pass filter.**

Fig. 6 shows the frequency response of the proposed 3-D BPF obtained with HFSS. For comparison, the results obtained from ideal 2th order Butterworth BPFs are given. Herein insertion loss S_{21} and return loss S_{11} represent signal attenuation and reflection as it passes through a filter, respectively, which are two important figures of merit for the electrical filter. For an ideal filter, it would have zero insertion loss in the pass-band and infinite attenuation in the stop-band. From these results, it is seen that the proposed filter meets the specifications for WLAN applications. The pass-band is centered at 2.45GHz with the FBW is 31.5%. The insertion loss is less than 2.4dB and the return loss is greater than 15dB. An extra transmission zero is found at 6.5GHz. Due to parasitic parameters in glass interposer and interconnects, a slight deviation between the above two filters is observed. Increasing TGV diameters and RDL cross-sectional area would be effective ways to improve the insertion loss characteristics of the proposed filter and decrease the deviation between these two filters. The underlying reason is that the increase in TGV diameters and RDL cross-sectional area can significantly decrease their equivalent resistance and corresponding loss of signal power.

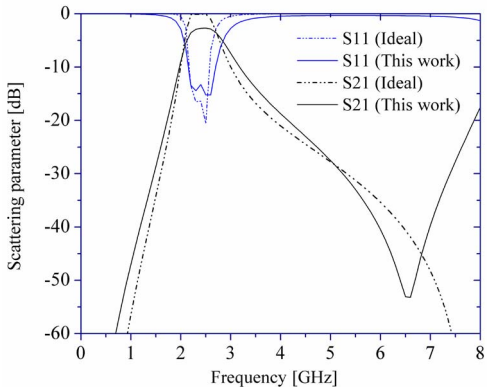

FIGURE 6. **Comparison of Scattering parameter.**

TABLE 2. **Performance comparison with some reported BPFs.**

	f_0 (GHz)	IL (dB)	RL (dB)	FBW (%)	Size (mm^2)	Technology
This work	2.45	2.4	15	31.5	0.44×0.33	TGV& RDL
[16]	2.33	0.65	15	39.8	18.5×18.5	Micro-strip line
[17]	2.5	0.3	17	70	39.9×5.6	
[18]	2.4	2.4	15	12.5	2.6×2.6	LTCC
[15]	2.45	2.2	12	36.2	1.1×2.3	
[20]	2.0	2.2	18	40.5	1.7×0.8	IPD
[21]	2.65	0.6	30	62.9	1×0.5	

Table 2 compares the performance of the proposed 3D BPF with respect to some reported filtering technology. In comparison with the filters with micro-strip line [16], [17] and LTCC technology [15], [18], it can be found that the proposed 3-D TGV filter has the noticeable advantages of a more compact size. This is attributed to the fact that the size of filters based on the transmission line structure is usually multiples of the quarter-wavelength. Using horizontal metal wires as on chip inductors and vertical through substrate vias as capacitors, various kinds of integrated passive devices have been proposed [19], [20] and [21]. Though the size advantage of the proposed filter is reduced as compared with the design based on the integrated passive device technology on a glass substrate [20], [21], the proposed filter exhibits lower fractional bandwidth and corresponding higher frequency sensitivity because of high quality factor of 3-D inductors.

IV. CONCLUSION

In this study, a TGV-based solenoid inductor is developed and the impact of various technical parameters on the electrical performance of the inductor is investigated. It is demonstrated that TGV inductors have high inductance and quality factor, which are appropriate as RF passive components. Based on the proposed TGV inductors and parallel plate capacitors, a coupled-resonator 2th band-pass filter is designed. Results show that the proposed filter has a more compact size in comparison with some reported BPFs and exhibits excellent filtering characteristics. Such a filter can be easily integrated into packages for miniaturized wireless communication system applications.

REFERENCES

[1] W. A. Vitale *et al.*, "Ultra fine-pitch TSV technology for ultra-dense high-Q RF inductors," in *Proc. Symp. VLSI Technol.*, Jun. 2015, pp. T52–T53, doi: 10.1109/VLSIT.2015.7223700.

[2] K. Dieng *et al.*, "Modeling and frequency performance analysis of through silicon capacitors in silicon interposers," *IEEE Trans. Compon. Packag. Manuf. Technol.*, vol. 7, no. 4, pp. 477–484, Apr. 2017, doi: 10.1109/TCPMT.2017.2655939.

[3] V. Sukumaran, T. Bandyopadhyay, V. Sundaram, and R. Tummala, "Low-cost thin glass interposers as a superior alternative to silicon and organic interposers for packaging of 3-D ICs," *IEEE Trans. Compon. Packag. Manuf. Technol.*, vol. 2, no. 9, pp. 1426–1433, Sep. 2012, doi: 10.1109/TCPMT.2012.2204392.

[4] J. Tong *et al.*, "Electrical modeling and analysis of tapered through-package via in glass interposers," *IEEE Trans. Compon. Packag. Manuf. Technol.*, vol. 6, no. 5, pp. 775–783, May 2016, doi: 10.1109/TCPMT.2016.2545160.

[5] S. Cho, V. Sundaram, R. R. Tummala, and Y. K. Joshi, "Impact of copper through-package vias on thermal performance of glass interposer," *IEEE Trans. Compon. Packag. Manuf. Technol.*, vol. 5, no. 8, pp. 1075–1084, Aug. 2015, doi: 10.1109/TCPMT.2015.2450731.

[6] X.-C. Wei, X.-J. Wang, D.-C. Yang, J. Li, and X. Wei, "Design of compact and low-EMI waveguide structures based on through glass vias," in *Proc. Int. Symp. Electromagn. Compat.*, Tokyo, Japan, May 2015, pp. 378–381.

[7] S. Hwangbo *et al.*, "Directional through glass via (TGV) antennas for wireless point-to-point interconnects in 3D integration and packaging," in *Proc. Electron. Compon. Technol. Conf.*, Orlando, FL, USA, Jun. 2017, pp. 260–265, doi: 10.1109/ECTC.2017.258.

[8] Y.-C. Hsieh, Y.-S. Chang, T. C. Lee, and C.-C. Wang, "Characterization of through glass via (TGV) RF inductors," in *Proc. Int. Microsyst. Packag. Assembly Circuits Technol. Conf.*, Taipei, Taiwan, 2016, pp. 87–90, doi: 10.1109/IMPACT.2016.7800071.

[9] J. Kim, R. Shenoy, K.-Y. Lai, and J. Kim, "High—Q 3D RF solenoid inductors in glass," in *Proc. IEEE Radio Freq. Integr. Circuits Symp.*, Tampa, FL, USA, 2014, pp. 199–200, doi: 10.1109/RFIC.2014.6851696.

[10] (2016). *Manual of HFSS V15*. [Online]. Available: https://www.ansys.com/products/electronics/ansys-hfss

[11] Z. Zhang and X. P. Liao, "Micromachined GaAs MMIC-based spiral inductors with metal shores and patterned ground shields," *IEEE Sensors J.*, vol. 12, no. 6, pp. 1853–1860, Jun. 2012, doi: 10.1109/JSEN.2011.2178066.

[12] H. K. Krishnamurthy *et al.*, "A 500MHz, 68% efficient, fully on-die digitally controlled buck voltage regulator on 22nm Tri-gate CMOS," in *VLSI Dig. Tech. Papers*, Jun. 2014, pp. 1–2, doi: 10.1109/VLSIC.2014.6858438.

[13] D.-H. Kim and Y.-J. Park, "Calculation of the inductance and AC resistance of planar rectangular coils," *Electron. Lett.*, vol. 52, no. 15, pp. 1321–1323, Jul. 2016, doi: 10.1049/el.2016.0696.

[14] D. M. Pozar, *Microwave Engineering*, 3rd ed. Hoboken, NJ, USA: Wiley, 2005.

[15] L. K. Yeung, K.-L. Wu, and Y. E. Wang, "Low-temperature cofired ceramic LC filters for RF applications," *IEEE Microw. Mag.*, vol. 9, no. 5, pp. 118–128, Oct. 2008, doi: 10.1109/MMM.2008.927634.

[16] J. Xu, "Compact quasi-elliptic response wideband bandpass filter with four transmission zeros," *IEEE Microw. Compon. Lett.*, vol. 25, no. 3, pp. 169–171, Mar. 2015, doi: 10.1109/LMWC.2015.2390571.

[17] C.-F. Chen, C.-Y. Lin, J.-H. Weng, and K.-L. Tsai, "Compact microstrip broadband filter using multimode stub-loaded resonator," *Electron. Lett.*, vol. 49, no. 8, pp. 545–546, Apr. 2013, doi: 10.1049/el.2012.4437.

[18] X. Y. Zhang *et al.*, "Compact LTCC bandpass filter with wide stopband using discriminating coupling," *IEEE Trans. Compon. Packag. Manuf. Technol.*, vol. 4, no. 4, pp. 656–663, Apr. 2014, doi: 10.1109/TCPMT.2013.2297522.

[19] F. Wang and N. Yu, "An ultracompact butterworth low-pass filter based on coaxial through silicon vias," *IEEE Trans. Very Large Scale Integr. (VLSI) Syst.*, vol. 25, no. 3, pp. 1164–1167, Mar. 2017, doi: 10.1109/TVLSI.2016.2620460.

[20] C.-H. Huang, Y.-C. Lin, T.-S. Horng, and L.-T. Hwang, "Design of compact bandpass filter using transformer-based coupled resonators on integrated passive device glass substrate," in *Proc. Asia–Pac. Microw. Conf.*, Melbourne, VIC, Australia, 2011, pp. 1921–1924.

[21] S. Sitaraman *et al.*, "Miniaturized bandpass filters as ultrathin 3-D IPDs and embedded thinfilms in 3-D glass modules," *IEEE Trans. Compon. Packag. Manuf. Technol.*, vol. 7, no. 9, pp. 1410–1419, Sep. 2017, doi: 10.1109/TCPMT.2017.2708704.

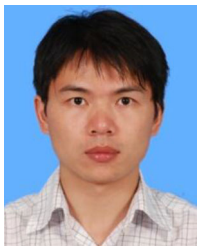

LIBO QIAN received the B.S. degree in electron-mechanics, and the M.S. and Ph.D. degree in electronics science and technology from Xidian University, Xi'an, China, in 2007, 2010, and 2013, respectively.

He currently serves as an Associate Professor with the Faculty of Electrical Engineering and Computer Science, Ningbo University. His current research interests include 3-D ICs based on the through silicon vias and signal integrity of high-speed interconnect circuits.

JIFEI SANG received the B.E. degree in communication engineering from Fuyang Normal University, Fuyang, China, in 2015. He is currently pursuing the M.E. degree with the Faculty of Electrical Engineering and Computer Science, Ningbo University.

YINSHUI XIA received the B.S. degree in physics and the M.S. degree in electronic engineering from Hangzhou University, Zhejiang, China, in 1984 and 1991, respectively, and the Ph.D. degree in electronic engineering from Edinburgh Napier University, Edinburgh, U.K., in 2003.

He was a Visiting Scholar with King's College London in 1999. He then joined Edinburgh Napier University as a Research Assistant and an Enterprise Fellow from 2000 to 2005. He is currently a Professor with Ningbo University, Ningbo, China. His research interests include low-power digital circuit design, logic synthesis and optimization, and SoC design.

JIAN WANG received the B.S. degree in mathematics and the M.S. degree in electronics engineering from Anhui University in 2004 and 2007, respectively, and the Ph.D. degree in electronics engineering from Shanghais Jiao Tong University in 2012.

He currently serves as an Associate Professor with the Faculty of Electrical Engineering and Computer Science, Ningbo University. His research interests include computational electromagnetic, electromagnetic compatibility, and low SAR antenna design for modern wireless mobile terminals.

PEIYI ZHAO received the B.S. degree in electronic engineering from Zhejiang University, Hangzhou, China, in 1987, and the Ph.D. degree in computer engineering from the University of Louisiana, Lafayette.

He was with Ningbo Radio Factory, Ningbo, China, from 1987 to 1995, designing FM/AM radio, television, and tape cassette recorder. From 1995 to 1999, he was with Ningbo Huaneng Corporation. He has been a Graduate Student Researcher in the VLSI Research Group, Center for Advanced Computer Studies, University of Louisiana, Lafayette, since 2001. Since 2005, he has been an Assistant Professor with Chapman University, Orange, CA, USA. He has one U.S. patent. His research interests include digital/analog circuit design, low power design, and digital VLSI design.